

AD-A103 531

REGIS COLL RESEARCH CENTER WESTON MA
FIELD-ALIGNED CURRENTS AND ELECTRIC FIELDS OBSERVED IN THE REGIS--ETC(U)
SEP 80 M A DOYLE, F J RICH, W J BURKE F1962B-80-C-0116
AFGL-TR-81-0236 NL

UNCLASSIFIED

1001
40-3544



END
DATE FILMED
40-811
DTIC

CTAFG KITR-81-0236

JOURNAL OF GEOPHYSICAL RESEARCH, VOL. 86, NO. A7, PAGES 5656-5664, JULY 1, 1981

AD A103531

Field-Aligned Currents and Electric Fields Observed in the Region of the Dayside Cusp

M. A. DOYLE AND E. J. RICH

Regis College Research Center, Weston, Massachusetts 02193

W. J. BURKE AND M. SMIDDY

Air Force Geophysics Laboratory, Hanscom Air Force Base, Bedford, Massachusetts 01731

DTIC
ELECTE

S AUG 31 1981

A

Thirteen passes of the S3-2 satellite, approximately along the noon-midnight meridian, during January 1976 through the region of the dayside cusp have been studied: eight in the northern hemisphere and five in the southern hemisphere. For all passes the IMF $B_z < 0$, and for all but three passes, $K_p \leq 3^-$, indicating relatively quiet times. Examination of the east-west component of the magnetic field deflections indicates an extra current sheet, located poleward of region 1 and carrying current in the opposite sense, on the postnoonside (prenoonside) in the northern (southern) hemisphere but no additional current prenoon (postnoon) in the northern (southern) hemisphere. The component of the convection electric field along the satellite trajectory (north-south) shows that convection reversals occur 2° - 3° equatorward of the boundary between this extra current sheet and the region 1 field-aligned current sheet. A boundary marking the transition from quasi-trapped to untrapped 100-keV protons was determined. The extra field-aligned current sheet lies almost entirely poleward of this transition boundary, suggesting that it may lie in a region of open magnetic field lines. Fine scale structure of the magnetic deflections indicates numerous field-aligned sheet and line currents embedded in the large-scale field-aligned current sheets.

INTRODUCTION

Field-aligned currents (FAC) along field lines from the magnetospheric equatorial plane and the magnetopause to the ionosphere have long been assumed to be important to the connection of the high-latitude ionosphere with the magnetosphere [Bostrom, 1964]. Field-aligned currents usually occur as sheets or regions with a much greater meridional extent than latitudinal extent, but line currents or regions of FAC with roughly equal meridional and latitudinal extent are also part of the connection. The TRIAD satellite measurements of magnetic field deflections have confirmed the existence of large-scale sheet currents along the auroral zone [Iijima and Potemra, 1976a]. In the poleward section of the auroral zone (region 1) the current is into (out of) the ionosphere on the morningside (eveningside). In the equatorward section of the auroral zone (region 2) the currents are reversed. Near midnight the TRIAD measurements indicate an overlap of morning and evening current systems similar to the overlap of convection patterns known as the Harang discontinuity. Near noon the early TRIAD results seemed ambiguous.

Recently, there has been considerable interest in the relationship between large-scale, field-aligned currents near the dayside cusp, high-latitude convection patterns, and the interplanetary magnetic field (IMF). A distinct set of FAC's has been observed from TRIAD measurements, poleward of the dayside, region 1 Birkeland current systems in both the northern [Iijima and Potemra, 1976b] and the southern [Iijima et al., 1978] hemisphere, and from rocket measurements [Primdahl et al., 1979]. These FAC's are most frequently observed between 0930 and 1430 MLT with a polarity that is opposite to that of the proximate region 1 system. Whether they appear in the prenoon or postnoon sector shows a two-to-one dependence on the hourly averaged value of the sign of the IMF B_z . In frequency of occurrence they are independent of B_z . They

are more intense, however, during periods when the IMF has a southward component.

Heelis et al. [1976] measured the convection pattern in the region of the dayside cusp, but they had no information about the associated field-aligned currents. McDiarmid et al. [1978a] have developed a technique for estimating the direction of ionospheric convection from the directions of transverse magnetic perturbations associated with FAC's. The method is applicable in places where the height-integrated Pedersen conductivity of the ionosphere has relatively high ($\Sigma_p \geq 1$ mho) and uniform values [Smiddy, et al., 1980], e.g., under sunlit conditions. McDiarmid et al. [1978b, 1979] have applied the method to study how magnetic field line tilts found near the cusp vary as a function of IMF B_z . In the northern hemisphere, $B_z > 0$ correlates with strong eastward deflections of the magnetic field near the poleward edge of the cusp, and $B_z < 0$ with strong westward deflections. The cusp region FAC's are interpreted as extensions of region 1 systems across the northern hemisphere, noon meridian into the prenoon (postnoon) sector for $B_z > 0$ ($B_z < 0$) [cf. McDiarmid et al., 1979, Figure 9]. As first suggested by Iijima and Potemra [1976b], the model shows a difference in the overlapping of regions 1 and 2 which depends on the direction of IMF B_z . Ground magnetometer measurements [Wilhelm and Friis-Christensen, 1978] show the existence of ionospheric currents located between two FAC sheets, determined from TRIAD measurements. The direction of this ionospheric current, assumed to be a Hall current, depends on the relative polarities of the FAC's and thus, too, on the sense of IMF B_z . Rostoker [1980] has found that the presence or absence of an eastward ionospheric current poleward of the westward current in the morning ionosphere is a function of the sign of IMF B_z .

Saflekos et al. [1979] attempted the first simultaneous observation of the electric field and magnetic field deflections using data from the Hawkeye 1 and TRIAD satellite, although the satellites were separated by approximately 2 hours in magnetic local time. For the two passes reported, electric field re-

versal and thus plasma convection reversal occurs colatitudinally with a reversal in the magnetic field deflection. It should be noted, however, that for only one pass did both satellites cross the polar cap on the same side of noon.

The purpose of this paper is to present a set of simultaneous measurements of the convective electric field (E) and transverse magnetic field deflections (ΔB) taken by instrumentation on the S3-2 satellite. Data were taken during 13 passes through the region of the dayside cusp in both the northern and the southern hemisphere. Particular attention is directed to the characteristics of the FAC lying poleward of region I and its relationship to the direction of the IMF. Available measurements from an energetic proton detector are used to locate the invariant latitude, at ionospheric altitudes, where the transition from quasi-trapped to untrapped 100-keV protons occurs. At the present time there is no universally accepted set of low-latitude signatures for the boundary between open and closed magnetic field lines [Heelis et al., 1980]. However, in this paper we use the boundary between quasi-trapped and untrapped 100-keV protons as a qualitative estimator of the open-closed field line boundary.

INSTRUMENTATION AND DATA PRESENTATION

The S3-2 satellite was launched into polar orbit during December 1975 with an initial apogee, perigee, and inclination of 1557 km, 240 km, and 96.3°, respectively. It was spin-stabilized, with a nominal spin period of 20 s and a spin axis that was nearly perpendicular to the orbital plane. During January 1976 the orbital plane was close to the noon-midnight meridian. Owing to the wobble of the magnetic dipole, data were sampled on both sides of magnetic noon.

The scientific package on S3-2 includes (1) an electric field experiment consisting of a 29.72-m dipole that lies in the spin plane of the satellite, (2) a triaxial flux-gate magnetometer, (3) an auroral electron spectrometer, and (4) an energetic positive ion spectrometer. The first three experiments are described in detail by Burke et al. [1980], and the fourth by Pantazis et al. [1975]. Components of the electric and magnetic field are presented in a satellite-centered coordinate system where X is in the spin plane of the satellite, perpendicular to the projection of the magnetic field into the spin plane, and positive along the satellite velocity; Z is parallel to the projection of the magnetic field into the spin plane and positive in the direction of nadir; and Y completes the right-hand system [cf. Smiddy et al., 1980, Figure 1]. Y is positive toward local west in the noon sector. Potential differences between the ends of the dipole are sampled 32 times per second and are presented as 5-s averages of E_x , or E_{forward} . Magnetic field measurements are taken at a rate of 32 samples/s with a 1-bit resolution of 5 nT. All of the data points are displayed as the difference between the measured and the international geomagnetic reference field (IGRF) 1975 model values of the spin axis component (ΔB_z). Only $E_x \approx E_{\text{north/south}}$ and $\Delta B_z \approx \Delta B_{\text{west}}$ are presented here because the meridional electric field component and the zonal magnetic field perturbation are the major auroral zone components [Kisabeth, 1979]. In the preparation of this paper, ΔB_z ($\Delta B_{\text{north/south}}$) has been examined, and its significance has been included in the discussion where necessary. The electron spectrometer measures electron fluxes in 32 energy channels between 80 eV and 17 keV, a full spectrum being compiled every second. The aperture is mounted in the spin plane of the satellite. Precipitating electrons in the auroral zone typically have energies of 1–10 keV; however, near the dayside cusp most of

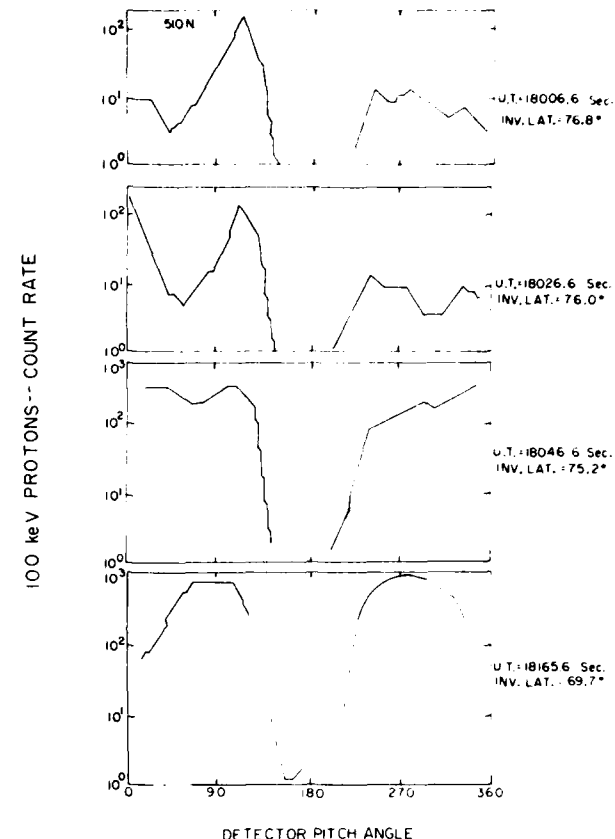


Fig. 1. Count rate for 100-keV protons versus detector pitch angle for four different times showing untrapped (18006.6, 18026.6 s), quasi-trapped (18046.6 s), and trapped (18165.6 s) protons. Pitch angles of 270° represent ions precipitating perpendicular to the magnetic field in the forward direction with respect to vehicle velocity or sunward.

the precipitating electrons have energies of ≤ 150 eV [McDiarmid et al., 1976]. Because of the small geometric factor of the instrument ($4.68 \times 10^{-5} \text{ cm}^2 \text{ sr}$), count rates are frequently at or below the one count per accumulation period ($\frac{1}{2}$ s). For this reason, electron flux measurements are only used as supplemental data. The energetic proton detector is a two-element solid-state telescope with a look direction in the satellite's spin plane. Electrons with energies < 600 keV are prevented from reaching the detector by a magnetic broom. The lowest discrimination level is nominally set to measure the flux of all protons with energies between 100 and 300 keV. One measurement is made per second, the full range of pitch angles being sampled once per satellite spin.

Available measurements from the energetic proton detector are used to determine the approximate position of a boundary between quasi-trapped and untrapped 100-keV protons as a qualitative estimator of the open-closed field line boundary. For example, in Figure 1 we have plotted the number of counts measured in the 100-keV channel of the positive ion spectrometer as a function of pitch angle during four spins of rev 510N. Electric and magnetic field measurements for this period are discussed below (Figure 4). To the right of each panel we have noted the universal time (UT), in seconds of the day, and the invariant latitude of the satellite at the beginning of each spin. The detector samples pitch angles that decrease with increasing time; i.e., 360° is sampled at the begin-

TABLE 1. Geophysical Conditions at or Near Times of S3-2 Passage Through the Region of the Dayside Cusp

S3-2 Orbit	IMF Data			
	B_x	B_y	B_z	K_p
<i>Northern Hemisphere</i>				
Prenoon				
420				2+
424 (+5 hours)	(-4.7)	(-0.6)	(-1.9)	2+
436 (+1 hour)	(3.1)	(-4.7)	(0.8)	2
605	5.0	-5.2	-2.0	4-
618 (-2 hours)	(4.8)	(-0.5)	(0.8)	2
Postnoon				
440	3.3	-5.1	-1.2	3-
510	6.3	-15.4	-3.5	5
629	3.1	-6.4	0.0	2+
<i>Southern Hemisphere</i>				
Prenoon				
424 (+5 hours)	(-4.7)	(-0.6)	(-1.9)	2+
629	1.2	-5.7	-1.0	2+
Postnoon				
436	3.1	-4.7	0.8	2
618 (1 hour)	(4.8)	(-0.5)	(0.8)	2+
801 (-2 hours)	(6.4)	(-5.6)	(1.4)	5+

ning and 0° at the end of a spin. Pitch angles of 270° (90°) represent ions precipitating perpendicular to the magnetic field and in the forward (backward) direction with respect to the vehicle velocity or sunward (antisunward). The spin commencing at 18006.6 UT is characterized by low proton count rates (≤ 10 per second) at all pitch angles. The high counts registered at pitch angles of $\sim 110^\circ$ are instrument responses to X rays emitted from nearby discrete auroral arcs. The sweep beginning at 18026.6 UT is similar to the previous one except that the count rate rises to > 100 c/s near 0° . This trend to high count rates continues in the third panel. Here proton fluxes are fairly isotropic over the downcoming hemisphere with a deep loss cone in the backscatter direction. These iso-

tropic pitch angle distributions continued to be measured to an invariant latitude of 69.7° , where the distribution became stably trapped (bottom panel). On the basis of these measurements the boundary between quasi-trapped and untrapped 100-keV protons precipitating at ionospheric altitudes is placed at $75.2^\circ \pm 0.8^\circ$. Since these protons are on field lines that are convecting poleward, this boundary in the equatorial plane is $\sim 0.5^\circ$ equatorward of the ionospheric position. Qualitatively, we estimate a lower limit on the position of the last closed field line to be 75.2° . We note that at this time, IMF $B_z = -3.5$ nT (Table 1). Thus 75.2° is approximately midway between the poleward and equatorward boundaries of the cusp expected for this IMF configuration [Burch, 1973].

Nine orbits (thirteen passes) approximately along the noon-midnight meridian during January 1976 were chosen for this study. These orbits were chosen because they fit the following criteria: (1) The orbit passed through the estimated position of the cusp, was directed approximately along a magnetic meridian, and reached a maximum invariant latitude of 80° or greater. (2) IMF data were available for the time of the orbit or within a few hours of the orbit. The trajectories of the satellite in invariant latitude and magnetic local time for these passes are given in Figure 2. Note that the satellite was moving southward on the dayside. In the northern hemisphere, five of the passes were prenoon and three were postnoon, while in the southern hemisphere, two were prenoon and three were postnoon. Table 1 summarizes geomagnetic data for each orbit. IMF data for the hour before (same hour) were used if the pass occurred in the first (last) half of the hour [King, 1979]. In cases where no IMF data were available, $(\pm t)$ indicates the number of hours before/after the pass when data were available. Purely by coincidence, IMF B_z was negative for all of the passes; IMF B_x was both negative and positive but never significantly large. Except for orbits 510, 605, and 801, when the K_p index was 5, 4-, and 5+, respectively, geomagnetic activity was low; that is, $K_p \leq 3-$.

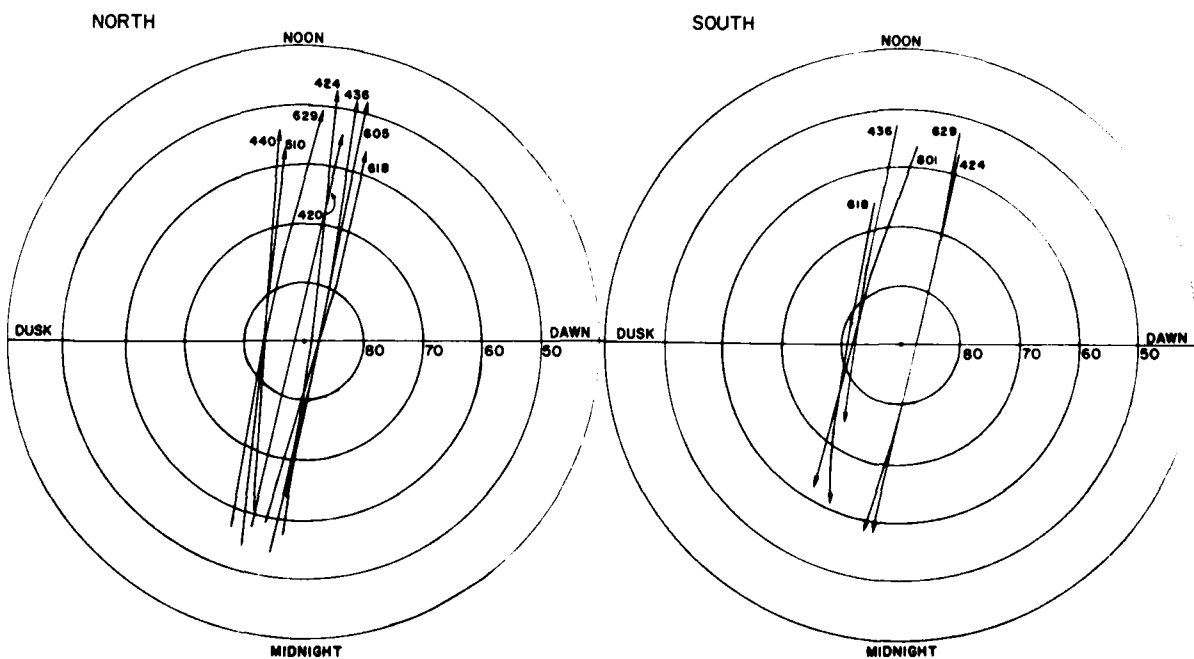


Fig. 2. Satellite trajectories for 13 passes of S3-2 during January 1976 through the region of the dayside cusp.

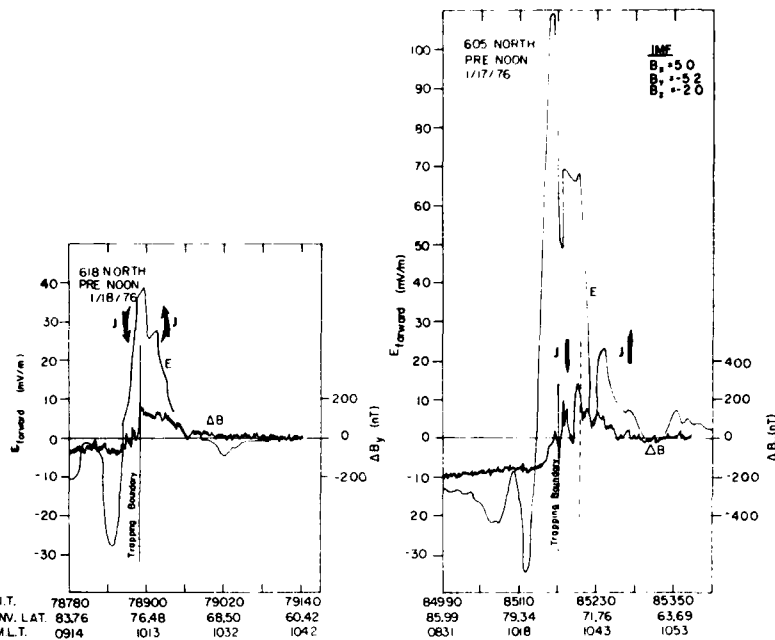


Fig. 3. Plots of the forward component of the electric field and the axial component of magnetic deflection as a function of universal time, invariant latitude, and magnetic local time for two northern hemisphere passes through the prenoon side of the dayside cusp. The solid (dashed) vertical line marks the boundary between quasi-trapped and untrapped 100-keV protons (boundary between current sheets).

Values of the forward component of the electric field (E_x) and the transverse magnetic field deflection measured during two prenoon passes in the northern hemisphere are given in Figure 3. Positive values of E_x represent a southward directed electric field component, while a positive ΔB_z represents westward deflections of the magnetic field. In both cases, ΔB_z has a predominantly westward deflection in the vicinity of the auroral zone corresponding to region 1 and region 2 Birkeland current sheets. During orbit 605 a fairly uniform eastward deflection of ~ 200 nT was found from the poleward edge of region 1 across the polar cap. In the case of orbit 618 this eastward deflection slowly increased from ~ 100 nT at the poleward boundary of region 1 to 200 nT on the nightside of the polar cap. A baseline for ΔB_z was determined by matching its low-latitude values on the dayside and nightside of the polar cap. Considerable structure is found in both region 1 and region 2 FAC's of orbit 605. North-south deflections of the magnetic field, smaller in magnitude, (not shown) were measured within these ΔB_z structures. These measurements indicate that the satellite passed through a series of sheet currents of finite extent, possibly containing embedded line currents. Although the flux of precipitating electrons is generally low, it shows a structural similarity to these smaller-scale currents. The dashed line in Figure 3 separates regions 1 and 2. In orbit 618 the boundary between the two regions is coincident with the boundary between quasi-trapped and untrapped 100-keV protons, indicated in all figures by a solid vertical line. To the left of this line the satellite was either near or in the region of open field lines. The westward deflection of the magnetic field due to the region 1/region 2 current system coincides with the region of generally sunward plasma flow. The transition from region 1 to a smooth polar cap magnetic deflection is coincident with the electric field reversal and hence antisunward plasma flow. While the transition bound-

ary between quasi-trapped and untrapped 100-keV protons is shown equatorward of the electric field reversal, it could be located as much as 1.3° poleward of the plotted value due to the time (20 s) required to obtain a pitch angle distribution. In that case the transition boundary for orbit 618 coincides with E field reversal and is only 0.7° equatorward of the reversal in orbit 605. The data are therefore consistent with a region 1/region 2 system located entirely on closed field lines convecting towards noon. Immediately poleward of the transition boundary the electron fluxes peak near 10^9 $(\text{cm}^2 \text{s sr})^{-1}$ in 605N and 2×10^8 $(\text{cm}^2 \text{s sr})^{-1}$ in 618N. These precipitating electrons have average energies ranging between 0.6 and 2.0 keV. Further poleward the flux level fell below the sensitivity of the detector.

Two north polar passes through the postnoonside of the cusp region (Figure 4) show generally three large-scale current sheets, two of which correspond to the region 1 and region 2 Birkeland current sheets. The extra current sheet, poleward of region 1, carries current into the ionosphere. In both cases the transition boundary from quasi-trapped to untrapped 100-keV protons is 0.5° poleward of the boundary between region 1 and this extra current sheet. Thus regions 1 and 2 lie on closed field lines, whereas the extra sheet may lie entirely on open field lines or may be partly in a region of open field lines. Flux levels measured by the electron spectrometer were too low to shed further light on whether field lines were open or closed. Small-scale current structures are observed in both passes. A region of sharply decreasing (current out) and increasing (current in) variations in ΔB_z was encountered near the transition boundary during orbit 629. Finally, we note that in both cases, E_x , and thus the east-west convective velocity component reversed directions $\sim 2.5^\circ$ equatorward of the boundary between region 1 and the extra current sheet.

Figure 5 is a plot of data that are representative of the cusp

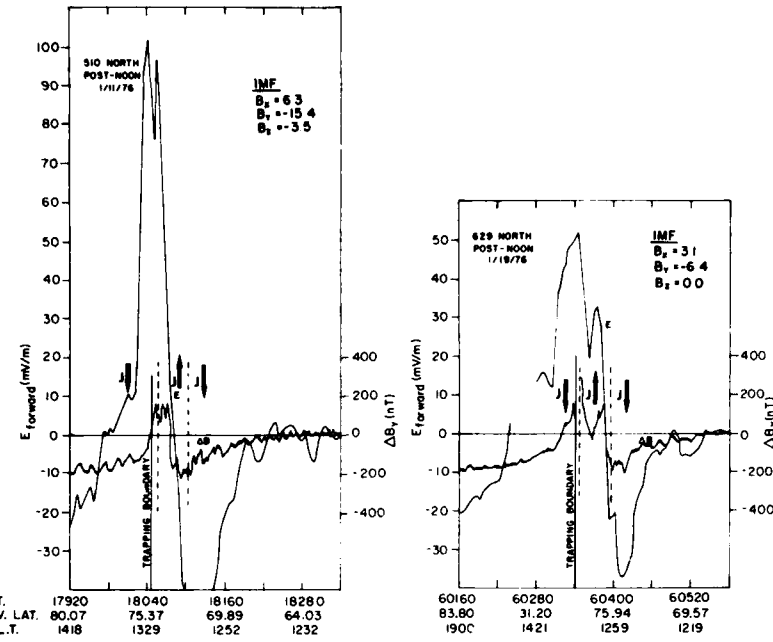


Fig. 4. Same as Figure 2 but for two northern hemisphere passes through the postnoonside of the dayside cusp.

region on both sides of noon in the southern hemisphere. Note that the data are plotted in a time reversed sense, so that the polar cap region is on the left side of the figure. Here we note two large-scale current systems, corresponding to regions 1 and 2 on the postnoonside, and three large-scale systems on the prenoonside. The E field reversal again occurs $\sim 3.0^\circ$

equatorward of the boundary between region 1 and the extra sheet of current flowing out of the ionosphere in the opposite sense as region 1. Since IMF B_y is negative for these passes, we expect the extra current sheet to be on the opposite side of noon from the northern hemisphere, as indeed it is. The transition boundary from quasi-trapped to untrapped 100-keV

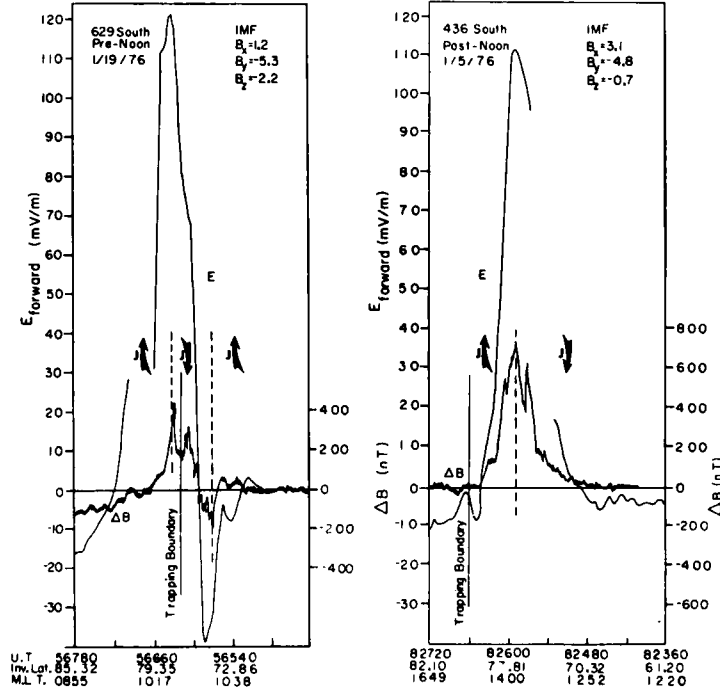


Fig. 5. Same as Figure 2 but for two southern hemisphere passes, one on either side of noon through the region of the dayside cusp. Data have been plotted in a time-reversed sense, so that the polar cap region is on the left.

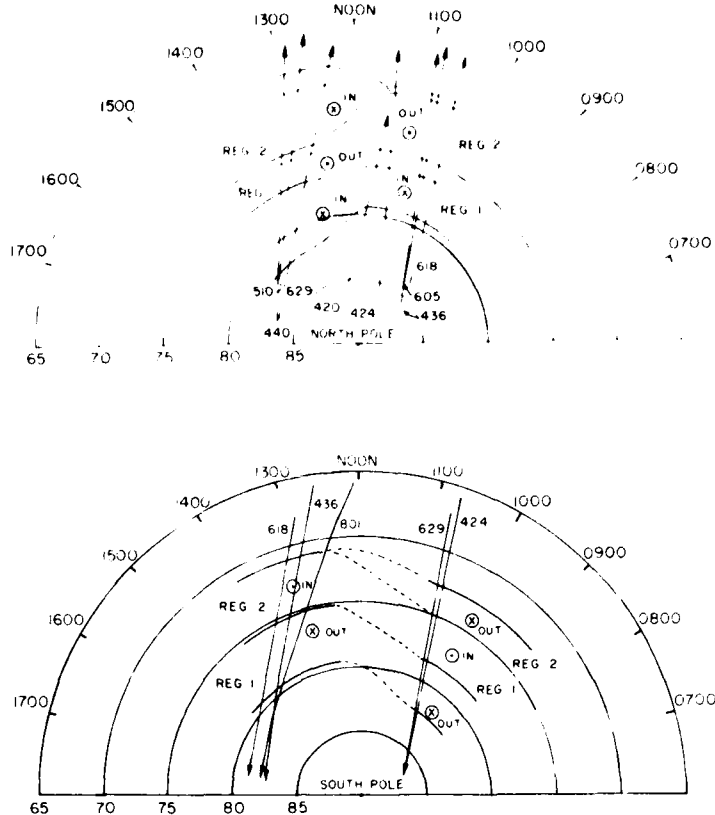


Fig. 6. Model showing an extra current sheet in the region of the dayside cusp on the postnoon side (prenoon side) of the northern (southern) hemisphere for an IMF $B_y < 0$. The perspective in the upper figure is looking down on the north pole, while in the lower figure it is looking through the earth at the south pole.

protons and the boundary between these two sheets are separated by 0.5° , placing the extra sheet almost entirely in a region of open field lines. Plasma convection is generally westward in this region. The postnoon pass shows only two current sheets, and we note that $E_v = 0$ and $\Delta B_v = 0$ are coincident, occurring 0.8° equatorward of the transition boundary. For this pass the electron spectrometer data show electrons precipitating into the ionosphere just poleward of the transition boundary with fluxes peaked about $3 \times 10^8 (\text{cm}^2 \text{s sr})^{-1}$ and energies from 1 to 2 keV.

DISCUSSION

On the basis of the 13 passes studied, average boundaries for regions 1 and 2 and the extra current sheet were determined for both hemispheres (Figure 6). The dashed lines are extrapolations of these boundaries across the noon meridian. The extra current sheet is then seen as an extension of region 1 across noon to the afternoonside (morningside) in the northern (southern) hemisphere. This agrees with the model of McDiarmid et al. [1979] for $B_z < 0$ and is consistent with the data presented by Saflekos et al. [1979]. It is quite possible that region 2 extends even further across the noon meridian than is shown, in which case an extra current sheet appears equatorward of region 2 on the opposite side of the noon as the extra poleward sheet. Our data give some evidence of this possibility as seen in Figures 7a and 7b. Figure 7a shows plots of E_v and ΔB_v for orbit 1698 on April 4, 1976. Note that the satellite crosses the noon meridian through the estimated posi-

tion of the dayside cusp. Clearly, there are three regions of field-aligned currents on the prenoon side. The extra field-aligned current sheet lies equatorward of region 2 and carries current into the ionosphere. We note in Figure 7b that this extra current sheet lies in a region of generally antisunward convection, as does region 2. Note that near local noon, equatorward of the boundary between open and closed field lines, antisunward convection in the ionosphere corresponds to sunward convection in the magnetospheric equatorial plane. It appears that from invariant latitude 78.7° to 76.0° the satellite crossed through the region of the postnoon extra field-aligned current sheet. We suggest that some of the earlier data of Iijima and Potemra [1976b] near noon could be interpreted as region 2 and an extra current sheet equatorward of region 2 rather than as region 1 and an extra sheet poleward. In that case their data would also show an IMF B_z dependence for the extra sheet rather than a prenoon/postnoon dependence. No passes along the noon-midnight meridian are presently available to establish how regions 1 and 2 on either side of noon meet one another. Therefore we assume a smooth overlapping of regions 1 and 2 such that the manner of overlapping depends on IMF B_z .

The convection velocity component perpendicular to the vehicle velocity, at 10-s intervals, is shown in Figures 8 and 9 for selected passes through the northern and southern hemispheres. This component of the convection velocity, obtained from E_v , is generally in the east-west direction. Lacking E_v data, we are unable to measure the north-south component of

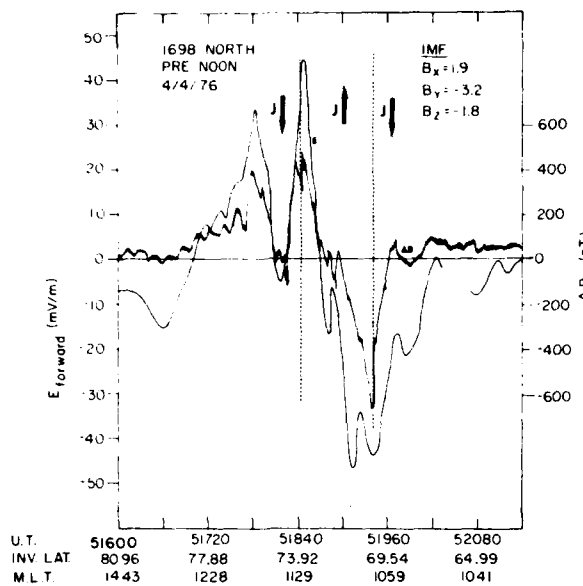


Fig. 7a. Plot of the forward component of the electric field and the axial component of magnetic deflection as a function of universal time, invariant latitude, and magnetic local time for orbit 1698 on April 4, 1976.

convection. However, we infer a general convection from the models of Heelis et al. [1976] and McDiarmid et al. [1979]. The convection velocity or convection electric field is larger in magnitude by a factor of 2–5 than that expected in the dusk or dawn sectors of the auroral zone for the same level of geomagnetic activity. Following the arguments of Heelis et al. [1976] this indicates that the convection flow contours or electric field equipotentials are drawn together near noon, so that all auroral zone convection passes through a relatively narrow region as it enters the dayside polar cap. Since most of the passes studied here have strong east-west convection on either side of a rapid change in E_x , we assume that these passes have missed any region of predominantly poleward flow. Thus any existing region of predominantly poleward flow must be confined to a small region in local time (≤ 1 hour). There is also a tendency for convection poleward of region 1 to be stronger in the region of the extra current sheet than in the region without current in the polar cap. This indicates that plasma entering the polar cap through the throat is 'pulled' or directed toward that flank of the polar cap containing the extra current sheet, as shown by the convective model of McDiarmid et al. [1979].

We also note that a maximum in the convection speed occurs at or near the boundary between regions 1 and 2. When the current sheet is extensive enough in local time and the height-integrated Pedersen conductivity is nearly constant throughout the region, this is consistent with the infinite current sheet approximation. In this case Maxwell's equation reduces to

$$\frac{\partial \Delta B_y}{\partial x} = \mu_0 \sum_p \frac{\partial E_x}{\partial x}$$

[cf. Smiddy et al., 1980, equation (6)]. Thus the maximum excursion in ΔB_y , which marks the boundary between regions 1 and 2, should also be the region of strongest east-west convection. Under sunlit conditions with low-energy electron pre-

cipitation the uniform conductivity condition is approximately satisfied.

Orbits 510N, 440N, and 424S exhibit an extra current sheet poleward of region 1, with a plasma convection reversal occurring at or near the boundary between these two regions. The largest difference ($\sim 2.5^\circ$) occurs in orbit 510N. However, the boundaries drawn represent the average location only, and the exact location may be dependent on other geophysical conditions—for example, the IMF B_z , as suggested by McDiarmid et al. [1978b]. The data support the contention that an extra current sheet, poleward of region 1 in the afternoon sector of the northern hemisphere, lies in a region of eastward convection, while in the southern hemisphere an extra current sheet, poleward of region 1 in the morning sector, lies in a region of westward plasma convection [Safekos and Potemra, 1980, and references therein].

The extra FAC system is always found poleward of the boundary between quasi-trapped and untrapped 100-keV protons. This implies that the extra FAC lies in or very near a region of open magnetic field lines, that is, the polar cap. Normally, polar cap convection is thought to be in the antisunward direction. However, Heppner [1972] showed that frequently the convection is not uniformly distributed across the polar cap. Depending on the sign of IMF B_z , the convective flow is often strongest near the dawn or dusk flank of the polar cap. With IMF $B_z < 0$, the strongest flow is found near the dawn flank of the southern or summer pole cap and is always near the dusk flank of the northern or winter pole cap. Recently, Crooker [1979] suggested that magnetic merging between the IMF and the earth's magnetic field occurs near the dayside cusp, where the fields are mostly antiparallel. With IMF $B_z < 0$, this is near the prenoonside (postnoonside) of the cusp in the northern (southern) hemisphere. Mechanical stresses exerted by the solar wind on newly merged field lines tend to drag the field lines toward the dusk (dawn) flank of the northern (southern) polar cap. In both hemispheres this drag appears as a southward directed electric field component. It should be strongest just poleward of the cusp in the postnoon (prenoon) sector of the northern (southern) hemisphere. This agrees with the S3-2 observations presented here.

It is interesting to compare the potential drop across the region of the extra FAC with the potential drop across the entire polar cap. As suggested by Heppner [1977], the potential drop

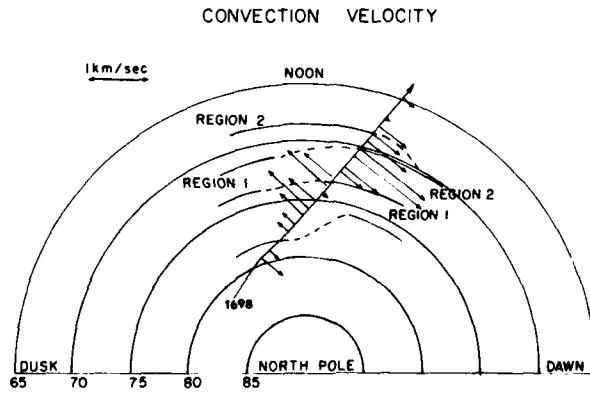


Fig. 7b. Plot of convection velocity as determined from the forward component of the E field in 20-s time intervals for the same orbit.

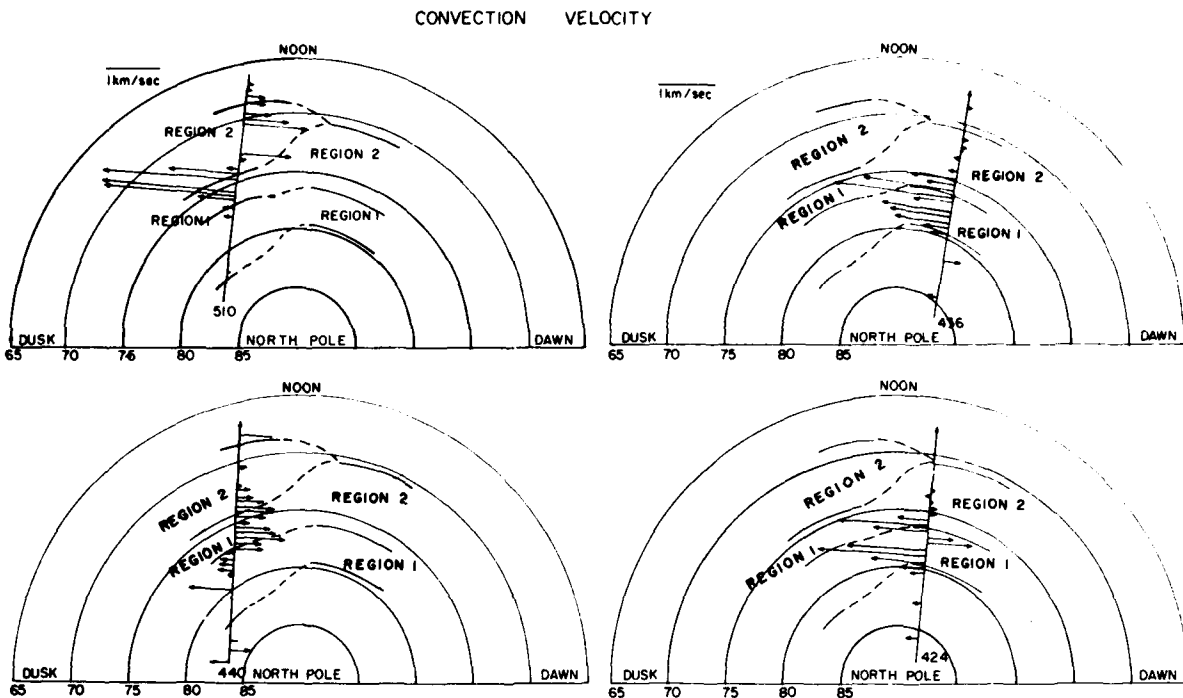


Fig. 8. Plots of convection velocity as determined from the forward component of the E field in 10-s time intervals for four passes in the northern hemisphere, two on either side of noon.

across the polar cap may be estimated by assuming $\Delta V = 20$ kV for $K_p = 0$ conditions, with a 20-kV increase for each integer change in K_p . For the five passes containing an extra current sheet poleward of region 1, the range of K_p indices from 2+ to 5 indicates polar cap potentials of 66–120 kV. Integrating $E_{\parallel} \cdot d\mathbf{l}$ across the region of the extra FAC, along the satellite trajectory, we note potential drops ranging from 14.1 to 31.0 kV. The largest ratio (0.47) of potential drop across the region of the extra FAC to potential drop across the polar cap occurred for orbit 424S.

The problem of conclusively determining whether the extra FAC lies on open or closed field lines remains. In a conducting ionosphere the southward electric field component for $B_z < 0$ will drive a Pedersen current toward (away from) the northern (southern) dayside cusp. To maintain a divergence-free current system, field-aligned currents of the opposite polarity to the cusp FAC must flow between the ionosphere and the generator of the cusp FAC. If the extra current system lies wholly or partially on open field lines, then it must close in the solar wind or on the magnetopause. The generator for the region 1/region 2 system is contained entirely in the closed field line portion of the magnetosphere [Smiddy et al., 1980]. Thus the extra field-aligned current, though contiguous with region 1, has an essentially different driving mechanism.

CONCLUSION

We chose orbits for which the convective electric field (E_{\parallel}), magnetic deflection (ΔB_{\parallel}) associated with field-aligned currents, and IMF data were readily available. In addition, 100-keV precipitating proton data enabled us to determine a boundary, marking the transition from quasi-trapped to untrapped protons. We are thus able to estimate a relative location for the region of open magnetic field lines, but we are not

able to determine a boundary for the last closed field line. The data show an extra FAC poleward of the region 1 Birkeland current sheet and this transition boundary; this implies that the extra FAC lies in (or very near) a region of open lines. For an IMF $B_z < 0$, this extra current sheet, carrying current into (out of) the ionosphere, appears on the postnoonside (pre-

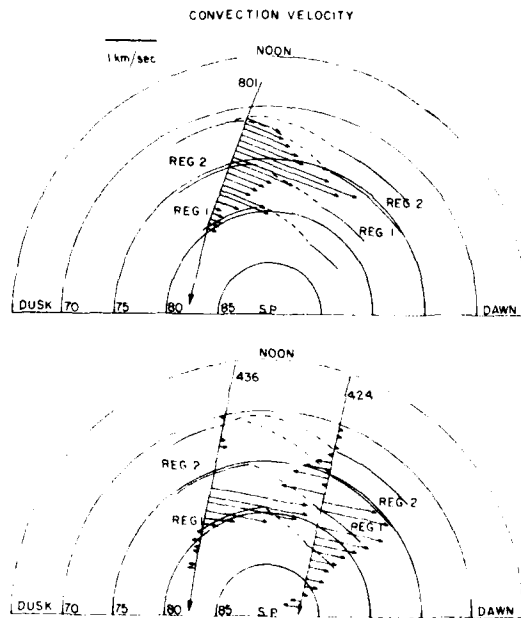


Fig. 9. Same as Figure 8 but for two passes in the southern hemisphere, one on either side of noon.

noonside) in the northern (southern) hemisphere. No additional FAC poleward of region I is apparent on the pre-noonside (postnoonside) in the northern (southern) hemisphere. This supports the model of McDiarmid *et al.* [1979], first suggested by Iijima and Potemra [1976a, b]. Although we have not presented any passes for an IMF $B_z > 0$, we expect the model (Figure 6) to be reversed for this case [McDiarmid *et al.*, 1979; Saflekos *et al.*, 1979].

The overlapping of current sheets depicted in the model is consistent with an extra current sheet equatorward of region 2 on the opposite side of noon as the extra FAC poleward of region 1. The data give some evidence of this possibility; however, this FAC is generally weak and not clearly distinguishable from a local line current embedded in region 2. Previously reported data (Iijima and Potemra, Iijima et al., McDiarmid et al., and Saflekos et al.) and our data support the model of an extra FAC poleward of region 1 on one side of noon or the other depending on the direction of IMF B_z , and an extra FAC equatorward of region 2 on the opposite side of noon. In the case of an extra equatorward FAC, there is no difficulty in considering it as an extension of the post-noon (prenoon) region 2 current sheet across noon in the northern (southern) hemisphere, since both region 2 and this extra FAC are contained entirely within the magnetosphere and presumably have the same generator. This is not true of the extra poleward FAC. In a region of open field lines the extra current closes somewhere in the solar wind or on the magnetopause.

A number of our passes contain significant small-scale structure indicating local line currents embedded in the large-scale FAC. The precipitating 0.1- to 17-keV electron data do occasionally verify the existence of these local line currents. It may be that the 'zone of confusion' in the dayside cusp referred to by *McDiarmid et al.* [1978b] is due to these numerous small-scale currents. The significance of these currents needs to be examined.

Acknowledgments. The authors wish to thank B. Shuman, R. P. Vancouver, and D. Smart of Air Force Geophysics Laboratory for providing S3-2 magnetic field, electron flux, and 100-keV flux measurements. This work was supported in part by USAF contract F19628-80-C-0116 with Regis College.

The Editor thanks G. Rostoker for his assistance in evaluating this paper.

REFERENCES

noonside) in the northern (southern) hemisphere. No additional FAC poleward of region 1 is apparent on the pre-noonside (postnoonside) in the northern (southern) hemisphere. This supports the model of McDiarmid et al. [1979], first suggested by Iijima and Potemra [1976a, b]. Although we have not presented any passes for an IMF $B_z > 0$, we expect the model (Figure 6) to be reversed for this case [McDiarmid et al., 1979; Saflekos et al., 1979].

The overlapping of current sheets depicted in the model is consistent with an extra current sheet equatorward of region 2 on the opposite side of noon as the extra FAC poleward of region 1. The data give some evidence of this possibility; however, this FAC is generally weak and not clearly distinguishable from a local line current embedded in region 2. Previously reported data (Iijima and Potemra, Iijima et al., McDiarmid et al., and Saflekos et al.) and our data support the model of an extra FAC poleward of region 1 on one side of noon or the other depending on the direction of IMF B_z , and an extra FAC equatorward of region 2 on the opposite side of noon. In the case of an extra equatorward FAC, there is no difficulty in considering it as an extension of the post-noon (prenoon) region 2 current sheet across noon in the northern (southern) hemisphere, since both region 2 and this extra FAC are contained entirely within the magnetosphere and presumably have the same generator. This is not true of the extra poleward FAC. In a region of open field lines the extra current closes somewhere in the solar wind or on the magnetopause.

A number of our passes contain significant small-scale structure indicating local line currents embedded in the large-scale FAC. The precipitating 0.1- to 17-keV electron data do occasionally verify the existence of these local line currents. It may be that the 'zone of confusion' in the dayside cusp referred to by McDiarmid et al. [1978b] is due to these numerous small-scale currents. The significance of these currents needs to be examined.

Acknowledgments. The authors wish to thank B. Shuman, R. P. Vancouver, and D. Smart of Air Force Geophysics Laboratory for providing S3-2 magnetic field, electron flux, and 100-keV flux measurements. This work was supported in part by USAF contract F19628-80-C-0116 with Regis College.

The Editor thanks G. Rostoker for his assistance in evaluating this paper.

REFERENCES

Bostrom, R., A model of the auroral electrojet, *J. Geophys. Res.*, 69, 4983, 1964.

Burch, J. L., Rate of erosion of dayside magnetic flux based on a quantitative study of the dependence of polar cusp latitude on the interplanetary magnetic field, *Radio Sci.*, 8, 955, 1973.

Burke, W. J., D. A. Hardy, F. J. Rich, M. C. Kelley, M. Smiddy, B. Shuman, R. C. Sagalyn, R. P. Vancouver, P. J. L. Wildman, and S. T. Lai, Electrodynamic structure of the late evening sector of the auroral zone, *J. Geophys. Res.*, 85, 1179, 1980.

Crooker, N. U., Antiparallel merging, the half-wave rectifier response of the magnetosphere, and convection, Proceedings of the Chapman Conference on Magnetospheric Boundary Layers, *ESA Spec. Publ.*, SP-148, Eur. Space Agency, Neuilly, France, 1979.

Heelis, R. A., W. B. Hanson, and J. L. Burch, Ion convection velocity reversals in the dayside cleft, *J. Geophys. Res.*, 81, 3803, 1976.

Heelis, R. A., J. D. Winnigham, W. B. Hanson, and J. L. Burch, The relationships between high-latitude convection reversals and the energetic particle morphology observed by Atmospheric Explorer, *J. Geophys. Res.*, 85, 3315, 1980.

Heppner, J. P., Polar cap electric field distributions related to the interplanetary magnetic field direction, *J. Geophys. Res.*, 77, 4877, 1972.

Heppner, J. P., Empirical models of high-latitude electric fields, *J. Geophys. Res.*, 82, 1115, 1977.

Iijima, T., and T. A. Potemra, The amplitude distribution of field-aligned currents at northern high latitudes observed by TRIAD, *J. Geophys. Res.*, 81, 2165, 1976a.

Iijima, T., and T. A. Potemra, Field-aligned currents in the dayside cusp observed by TRIAD, *J. Geophys. Res.*, 81, 5971, 1976b.

Iijima, T., R. Fujii, T. A. Potemra, and N. A. Saflekos, Field-aligned currents in the south polar cusp and their relationship to the interplanetary magnetic field, *J. Geophys. Res.*, 83, 5595, 1978.

King, J. H., Interplanetary medium data book supplement I 1975-1978, *Publ. NSSDC/WDC-A-R&G79-08*, Goddard Space Flight Center, Greenbelt, Md., 1979.

Kisabeth, On calculating magnetic and vector potential fields due to large-scale magnetospheric current systems and induced currents in an infinitely conducting earth, in *Quantitative Modelling of Magnetospheric Processes*, edited by W. P. Olson, AGU, Washington, D. C., 1979.

McDiarmid, I. B., J. R. Burrows, and E. E. Budzinski, Particle properties in the dayside cleft, *J. Geophys. Res.*, 81, 221, 1976.

McDiarmid, I. B., J. R. Burrows, and M. D. Wilson, Comparison of magnetic field perturbations at high latitudes with charged particle and IMF measurements, *J. Geophys. Res.*, 83, 681, 1978a.

McDiarmid, I. B., J. R. Burrows, and M. D. Wilson, Magnetic field perturbations in the dayside cleft and their relationship to the IMF, *J. Geophys. Res.*, 83, 5753, 1978b.

McDiarmid, I. B., J. R. Burrows, and M. D. Wilson, Large-scale magnetic field perturbations and particle measurements at 1400 km on the dayside, *J. Geophys. Res.*, 84, 1431, 1979.

Pantazis, J., A. Huber, and M. P. Hagan, Design of a low-energy proton spectrometer, final report (Emmanuel College), *Rep. AFCRL-TR-75-0637*, Air Force Cambridge Res. Lab., Bedford, Mass., 1975.

Primdahl, F., J. K. Walker, F. Spanglev, J. K. Olesen, U. Fahleson, and E. Ungstrup, Sunlit cleft and polar cap ionospheric currents determined from rocket-borne magnetic field, plasma, and electric field observations, *J. Geophys. Res.*, 84, 6458, 1979.

Rostoker, G., Magnetospheric and ionospheric currents in the polar cusp and their dependence on the B_z component of the interplanetary magnetic field, *J. Geophys. Res.*, 85, 4167, 1980.

Saflekos, N. A., and T. A. Potemra, The orientation of Birkeland current sheets in the dayside polar region and its relationship to the IMF, *J. Geophys. Res.*, 85, 1987, 1980.

Saflekos, N. A., T. A. Potemra, P. M. Kintner, Jr., and J. L. Green, Field-aligned currents, convection electric fields, and ULF-ELF waves in the cusp, *J. Geophys. Res.*, 84, 1391, 1979.

Smiddy, M., W. J. Burke, M. C. Kelley, N. A. Saflekos, M. S. Gussenhoven, D. A. Hardy, and F. J. Rich, Effects of high-latitude conductivity on observed convection electric fields and Birkeland currents, *J. Geophys. Res.*, 85, 6811, 1980.

Wilhelm, J., E. Friis-Christensen, and T. A. Potemra, The relationship between ionospheric and field-aligned currents in the dayside cusp, *J. Geophys. Res.*, 83, 5586, 1978.

(Received September 22, 1980;
revised December 31, 1980;
accepted January 29, 1981.)

Unclassified

SECURITY CLASSIFICATION OF THIS PAGE(When Data Entered)

(postnoon) in the northern (southern) hemisphere. The component of the convection electric field along the satellite trajectory (north-south) shows that convection reversals occur 2° - 3° equatorward of the boundary between this extra current sheet and the region 1 field-aligned current sheet. A boundary marking the transition from quasi-trapped to untrapped 100 keV protons was determined. The extra field-aligned current sheet lies almost entirely poleward of this transition boundary, suggesting that it may lie in a region of open magnetic field lines. Fine scale structure of the magnetic deflections indicates numerous field-aligned sheet and line currents embedded in the large scale field-aligned current sheets.

Unclassified

SECURITY CLASSIFICATION OF THIS PAGE(When Data Entered)

Unclassified

SECURITY CLASSIFICATION OF THIS PAGE (When Data Entered)

REPORT DOCUMENTATION PAGE		READ INSTRUCTIONS BEFORE COMPLETING FORM
1. REPORT NUMBER AFGL-TR-81-0236	2. GOVT ACCESSION NO.	3. RECIPIENT'S CATALOG NUMBER
4. TITLE (and Subtitle) Field-Aligned Currents and Electric Fields Observed in the Region of the Dayside Cusp		5. TYPE OF REPORT & PERIOD COVERED Reprint Scientific, Interim
7. AUTHOR(s) M.A. Doyle, F.J. Rich W.J. Burke,* M. Smiddy*		6. PERFORMING ORG. REPORT NUMBER 2
9. PERFORMING ORGANIZATION NAME AND ADDRESS Regis College Research Center 235 Wellesley Street Weston, MA 02193		10. PROGRAM ELEMENT, PROJECT, TASK AREA & WORK UNIT NUMBERS 61102F 2311G2CA
11. CONTROLLING OFFICE NAME AND ADDRESS Air Force Geophysics Laboratory Hanscom AFB, MA 01731 Susan Bredesen/PHC/Monitor		12. REPORT DATE July 1, 1981
14. MONITORING AGENCY NAME & ADDRESS (if different from Controlling Office)		13. NUMBER OF PAGES 9
		15. SECURITY CLASS. (of this report) Unclassified
		15a. DECLASSIFICATION DOWNGRADING SCHEDULE
16. DISTRIBUTION STATEMENT (of this Report) Approved for public release; distribution unlimited		
17. DISTRIBUTION STATEMENT (of the abstract entered in Block 20, if different from Report)		
18. SUPPLEMENTARY TES *Air Force Geophysics Laboratory Hanscom AFB, MA 01731		
19. KEY WORDS (Continue on reverse side if necessary and identify by block number) Field-aligned currents Ionosphere Electric fields Dayside cusp		
20. ABSTRACT (Continue on reverse side if necessary and identify by block number) Thirteen passes of the S3-2 satellite, approximately along the noon-midnight meridian, during January, 1976 through the region of the dayside cusp have been studied: eight in the northern hemisphere and five in the southern hemisphere. For all passes the IMF $B < 0$, and for all but three passes $K_p \leq 3$, indicating relatively quiet times. Examination of the east-west component of the magnetic field deflections indicates an extra current sheet, located poleward of region 1 and carrying current in the opposite sense, on the postnoon (prenoon) side in the northern (southern) hemisphere but no additional current prenoon		

DD FORM 1 JAN 73 1473

Unclassified

SECURITY CLASSIFICATION OF THIS PAGE (When Data Entered)

FILME

